ELSEVIER

Spectrochimica Acta Part B 62 (2007) 1237 – 1245

SPECTROCHIMICA ACTA PART B

www.elsevier.com/locate/sab

Measurement of Stark broadening of Mn I and Mn II spectral lines in plasmas used for Laser-Induced Breakdown Spectroscopy

F. Bredice [a], F.O. Borges [b], H. Sobral [c], M. Villagran-Muniz [c], H.O. Di Rocco [d], G. Cristoforetti [e], S. Legnaioli [e], V. Palleschi [e,*], A. Salvetti [e], E. Tognoni [e]

[a] *Centro de Investigaciones Opticas, P.O.Box 124, (1900) La Plata, Argentina*
[b] *Instituto de Física, Universidade Federal Fluminense, UFF, Campus da Praia Vermelha-Gragoatá, 24210-340 Niterói, Rio de Janeiro, Brazil*
[c] *Laboratorio de Fotofísica, Centro de Ciencias Aplicadas y Desarrollo Tecnológico, Universidad Nacional Autónoma de México, Apartado Postal 70-186 México Distrito Federal, PO Box 04510, Mexico*
[d] *Instituto de Física "Arroyo Seco", Facultad de Ciencias Exactas, U.N.C.P.B.A., Pinto 399, 7000 Tandil, Argentina*
[e] *Applied Laser Spectroscopy Laboratory, IPCF-CNR, Area della Ricerca di Pisa, Via G. Moruzzi 1, 56124 Pisa — Italy*

Received 21 June 2007; accepted 8 October 2007
Available online 17 October 2007

Abstract

We present measurements of the Stark broadening of several Mn lines in the conditions of typical laser-induced plasmas. Single-and double-pulse Laser-Induced Breakdown spectroscopy (LIBS) configurations are studied on a series of Fe–Mn alloy samples with Mn concentration ranging from 6% to 30%. The effects of self-absorption on the measured line broadenings are discussed in detail. In particular, the experimental results evidence that self-absorption is much higher in laser-induced plasmas generated with double pulses, compared to the case of single pulse. After measurement of the electron density, the Stark coefficients of several neutral and ionic Mn lines are derived through the measure of the broadening in conditions of optically thin plasma. The results obtained for singly ionized Mn lines are compared with the theoretical and experimental data present in the literature. For the first time, experimental measurements of the Stark coefficient for several neutral Mn lines are also presented.

Keywords: Stark broadening; LIBS; Self-absorption; Fe–Mn alloys; Double pulse

1. Introduction

The knowledge of the Stark coefficients of atomic emission lines is of paramount importance in many different fields, ranging from astrophysics to analytical chemistry [1–4].

The determination of these coefficients is usually carried out using arc discharges, Z-pinch plasmas, or electromagnetically driven T tubes [5–10]. In a recent paper [11] Bengoechea et al. proposed the use of Laser-Induced Breakdown Spectroscopy (LIBS) for measuring the Stark coefficient of emission lines, demonstrating that an accuracy of the order of 7% on the determined Stark coefficient can be obtained in LIBS experiments. For reaching this level of accuracy, the possible occurrence of self-absorption [12] in the plasma should be excluded; in fact, it has been demonstrated that self-absorption effects could lead to an over-estimation of the Stark coefficient [13].

In this paper we used LIBS for the measure of the Stark coefficients of the same Mn II lines studied by Djeniže et al. in Ref. [14], in conditions which are typical of laser induced plasmas. We followed an approach similar to the one described in Ref. [11], using a series of Fe–Mn certified samples with Mn concentration ranging from 6% to 30%.

The study of Fe–Mn alloys is extremely important, for example, in shape-memory alloys applications [15–19]. However, the knowledge of Mn line broadening coefficient is also interesting in astrophysics, see for example Ref. [14,20].

* Corresponding author.
E-mail address: vince@ipcf.cnr.it (V. Palleschi).

0584-8547/$ - see front matter © 2007 Elsevier B.V. All rights reserved.
doi:10.1016/j.sab.2007.10.014

Several theoretical calculations and experimental measurements on Mn II line broadening in plasmas have been recently published. The measurements by Djeniže et al. [14] were performed on Mn II lines at a plasma temperature of about 50,000 °K, therefore they can be considered just as a order-of-magnitude reference for the results obtained in typical LIBS conditions, where the temperatures are around 10,000 K. However, it is interesting comparing these results with the prediction of theoretical calculations, presented by Popović and Dimitrijević [20]. As stated by the authors, the Djeniže measurements show substantial deviations (by a factor ranging from 3 to 6, depending on the line considered) from the theoretical predictions.

In the following section the theoretical background underlying this work is briefly recalled. The dominant mechanism of line broadening in laser-induced plasmas and the effects of optical thickness on the line profile are described. Section 3 reports an estimation of the effects of plasma inhomogeneity on the measured line broadening. The conditions of measurement are then described and the results presented and discussed.

2. Theoretical background

2.1. Broadening of emission lines in plasmas

The observed lineshape of atomic and ionic emission lines in plasmas is the result of many different physical effects, such as resonance, Van der Waals, Stark and Doppler broadening (for a detailed discussion of these effects, see for example Ref. [21]). However, in typical laser-induced plasmas the dominant effect is related to the interaction of the radiating atoms with the electric micro-field generated by the surrounding electrons and ions (Stark effect). The Stark effect is responsible of a broadening of the plasma emission lines, according to the following equations [21]:

$$w(n_e, T) = 2w_s(T)\left[1 + gA(T) \times 10^{-4}\right]n_e \times 10^{-16} \quad (1)$$

for neutral lines or

$$w(n_e, T) = 2w_s(T)n_e \times 10^{-17} \quad (2)$$

for ionic lines.

In the previous expressions w corresponds to the full-width at half maximum (FWHM) of the emission line, w_s is the Stark coefficient for the given line, weakly dependent on temperature, g (dimensionless)=1.75 (1–0.75R), with R being the Debye shielding parameter and n_e (cm^{-3}) is the electron density. A (dimensionless) is a parameter related to the effect of electric micro-field produced on the emitter by the surrounding ions. In many practical cases the effect of ionic perturbers on the emitter can be safely neglected. In this case, the Eqs. (1) and (2) become identical for neutral and ionic lines; when the ionic broadening is negligible, the Stark coefficient w_s corresponds to the half width at half maximum (HWHM) of the emission line at plasma electron density $n_e=10^{16}$ cm^{-3} for neutral lines and at $n_e=10^{17}$ cm^{-3} for the emission lines of singly charged ions.

In view of Eqs. (1) and (2), the measurement of Stark broadening in laser-induced plasmas seems to be a trivial task, provided that electron density and temperature are known by independent measurements. However, self-absorption effects and plasma inhomogeneity may affect the apparent line profile, which is measured by integration along the line of sight. Thus systematic errors in the determination of the Stark parameter may arise from the use of Eqs. (1) or (2).

2.2. Self-absorption of emission lines in plasmas

In this section we recall the basic treatment of self-absorption in laser-induced plasmas and derive the expression for its contribution to line broadening, as stated in a previous paper of the authors [13].

According to the two-levels treatment of atomic emission, the number of photons emitted per unit time at wavelength λ by a homogeneous plasma rod of length l (cm) and unit section surface at Local Thermal Equilibrium can be written in the form

$$n_p(\lambda, l) = \frac{\varepsilon(\lambda)}{\kappa(\lambda)}\left(1 - e^{-\kappa(\lambda)l}\right) \quad (3)$$

where $\varepsilon(\lambda)$ and $\kappa(\lambda)$ represent respectively the number of photons emitted per unit time, volume and wavelength (s^{-1} cm^{-4}) and the absorption coefficient (cm^{-1}), and can be in turn expressed by

$$\varepsilon(\lambda) = \frac{1}{4\pi}A_{ki}g_k n_0 \frac{e^{-\frac{E_k}{k_B T}}}{U(T)}L(\lambda) \quad (4)$$

and

$$\kappa(\lambda) = \frac{\lambda_0^4}{8\pi c}A_{ki}g_k \frac{n_0 e^{-\frac{E_i}{k_B T}}}{U(T)}L(\lambda) \quad (5)$$

where c is the speed of light (cm s^{-1}), g_k is the degeneracy of the upper level (dimensionless), λ_0 is the central wavelength of the transition (cm), A_{ki} represents the transition probability between the upper level k and the lower level i (s^{-1}), n_0 is the number density of the species considered (cm^{-3}), E_i and E_k are the energy (erg) of the lower and the upper levels respectively, k_B is the Boltzmann constant (erg K^{-1}), T is the plasma temperature (K), $U(T)$ is the partition function (dimensionless) for the species and $L(\lambda)$ is the spectral emission profile (cm^{-1}).

For temperature and electron density values which are typical in the laser-induced plasmas, the Stark broadening of the line is usually dominant over any other effect, thus we assume that the emission line $L(\lambda)$ (in the absence of self-absorption) has a pure Lorentzian profile, i.e.

$$L(\lambda) = \frac{\Delta\lambda_0}{4(\lambda - \lambda_0)^2 + \Delta\lambda_0^2} \quad (6)$$

where $\Delta\lambda_0$ represents the FWHM of the line. The use of Lorentzian line shape is appropriate when the ion static contribution to the Stark broadening is negligible [22]. In this case the linewidth $\Delta\lambda_0$ is approximately proportional to the plasma electron density n_e through the temperature dependent

Stark coefficient w_s (see Eqs. (1) or (2)). It should be noted that, even in the absence of self-absorption effects, the experimentally recorded line profile might be affected by other line broadening mechanisms (such as Doppler broadening and/or instrumental broadening) so that the resulting experimental lineshape is better represented as a Voigt profile.

In order to characterize the effect of self-absorption on the shape and intensity of a given emission line, in a previous paper [12] we introduced the self-absorption coefficient SA, defined as the ratio of the observed line intensity (in counts per seconds) at its maximum over the same intensity obtained through linear extrapolation at the actual elemental concentration of the linear part of the curve-of-growth obtained in the limit of low opacity ($\kappa(\lambda_0)l \ll 1$)

$$\mathrm{SA} = \frac{n_p(\lambda_0)}{n_{p_0}(\lambda_0)} = \frac{\left(1 - e^{-\kappa(\lambda_0)l}\right)}{\kappa(\lambda_0)l} \tag{7}$$

It was demonstrated [12] that the ratio of the integral intensity of the self-absorbed emission line over the non self-absorbed one (extrapolated as above described) scales as

$$\frac{N_p}{N_{p_0}} = \frac{\int n_p(\lambda)d\lambda}{\int n_{p_0}(\lambda)d\lambda} = (\mathrm{SA})^{\beta} \tag{8}$$

with $\beta = 0.46$, while the FWHM of the measured emission line becomes

$$\Delta\lambda = \Delta\lambda_0(\mathrm{SA})^{\alpha} \tag{9}$$

with $\alpha = \beta - 1 = -0.54$.

The last expression is exploited in the following to give an interpretation of the experimental results and in particular of the observed broadening of the emission lines.

3. Effect of plasma inhomogeneity on the emission lines profiles

The general treatment of Stark effect and self-absorption in plasma assumes that the emitting plasma is homogeneous. However, when LIBS plasmas are used as the emitting source for experimental determination of Stark coefficients, spatial inhomogeneities may affect the results of line width measurement. Recently, a maximum discrepancy of about 7% has been reported among the values of Stark broadening parameter obtained from spatially-integrated and spatially-resolved measurements in laser-induced plasmas [11]. Unfortunately, the generalization of these encouraging results to any LIBS measurement cannot be taken for granted, due to the differences in experimental conditions, which are likely to produce plasmas with very different properties. Therefore, we decided to evaluate the order of magnitude of the effect of plasma inhomogeneity on the apparent linewidth for our experimental conditions. Using the Matlab® environment, we wrote a code to implement the radiation transport equations described in Section 2.2 in a generic inhomogeneous plasma. We considered a pure Mn plasma, with density $n_0 = 10^{14}$ particles/cm^3. The LIBS plasma was represented as a rod with total length $l_0 = 0.2$ cm. The one-dimensional radiation transport along the rod length was only considered, therefore the surface of the rod is not influencing the results (its effect is just a scale factor in the emission intensity). The spatial distribution of the plasma parameters (temperature, Mn particle density and electron density) within the plasma rod was assumed constant in the interval $-l_0/2 \le -l'/2 \le x \le +l'/2 \le +l_0/2$ and then linearly decreasing down to zero at $x = \pm l_0/2$. This model is based on a simplified representation of the experimental results obtained by three-dimensional mapping of the plasma as reported by the authors in Ref. [23]. We would like to stress again that the computer simulation is far from giving a real representation of the plasma emission, which is in fact intrinsically three-dimensional; however, the choice of reasonable plasma parameters and dimensions allows giving at least an order of magnitude of the effect of self-absorption in non-homogeneous plasmas. In the simulation, a homogeneous plasma would correspond to $l'/l_0 = 1$. The parameter l' can be set at will, and the corresponding emission profile resulting from the integration along the line of sight is calculated.

For the code to operate, the spectral parameters and the Stark broadening coefficient of the emission lines considered should be available. At that purpose, we used for the Stark broadening coefficients the values actually measured in our experiment (see following section). The spectral parameters of the lines considered are taken from atomic and spectroscopic databases [24,25].

For giving an example of the code output, the simulated profile of the three Mn II emission lines at 293.31, 293.93 and 294.92 nm is shown in Fig. 1. The laser plasma is assumed homogeneous ($l'/l_0 = 1$) in this simulation. The figure also shows the experimental LIBS spectrum in the same wavelength interval. Note that the plasma parameters used in the simulation correspond to the ones experimentally measured from the LIBS spectrum; the only free parameter is the scale factor of the simulated spectrum.

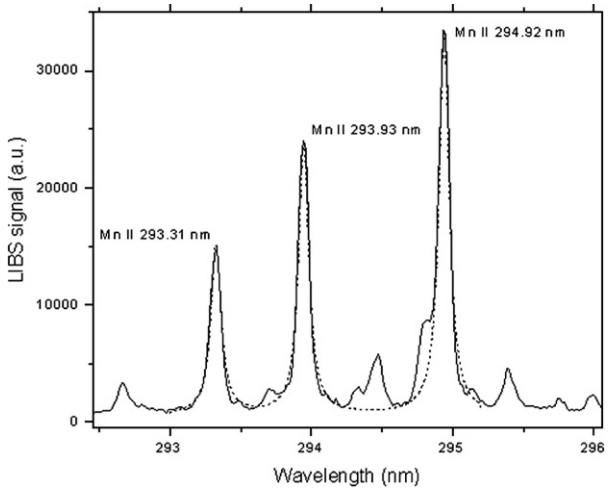

Fig. 1. Comparison between experimental LIBS spectrum (solid line — Fe–Mn sample (Mn 6%) single pulse, 120 mJ laser energy, 1 μs acquisition delay and 500 ns gate) and simulated spectrum (dashed line, $T = 1.25$ eV, $n_e = 4.3 \times 10^{17}$, $n_0 = 10^{14}$ particles/cm^3).

It is evident from the inspection of the figure that the homogeneous plasma approximation seems to be well adequate for reproducing the experimental profile, at least for the lines here considered.

However, changing the 'homogeneity' parameter l'/l_0 causes the predicted line width to change. In our model, in fact, the plasma is composed of an internal homogeneous core and an external shell where the Mn particles density, electron density and the temperature decrease linearly toward atmospheric values. Changing the ratio l'/l_0 corresponds to change the relative weight of the homogeneous core and inhomogeneous shell.

Let's define w_0 as the predicted FWHM of the Mn II line at 293.31 nm in case of homogeneous plasma ($l'/l_0=1$, as in Fig. 1) and w' as the predicted FWHM of the same line in the generic non-homogeneous case.

Fig. 2 shows the dependence of the ratio w'/w_0 on the parameter l'/l_0. Similar results, not shown here, were obtained for the other Mn lines considered in the current work. The plasma parameters used for this simulation are the same as for the simulation shown in Fig. 1.

According to our model, an inhomogeneity parameter of 0.2 in the plasma – which indeed seems a quite pessimistic representation of the real situation – gives a linewidth which is lower by only 3% than the value corresponding to a homogeneous plasma.

In any case, as already stated at the beginning of the discussion, no conclusive information can be gathered by the simulation unless a serious estimate of the plasma homogeneity is given. The results here presented are intended to give just a rough indication of the effects of plasma inhomogeneity; a more detailed work specifically devoted to this problem will be published in a forthcoming paper. In the current measurements, plasma inhomogeneity is neglected.

4. Experimental results and discussion

The line broadening measurements were performed on a series of Fe–Mn samples with Mn concentration ranging from 30 to 6% in weight, at ALS Lab in Pisa. The measurements were done using Modì (MObile Dual-pulse Instrument), a double-pulse mobile LIBS system realized by the Applied Laser Spectroscopy group in collaboration with Marwan Technology s.r.l. (Pisa) [26]. Modì uses a Nd-YAG Laser emitting two collinear pulses (with a reciprocal delay variable from 0 to 50 μs) at 1064 nm with 60 mJ energy per pulse and 12 ns FWHM, coupled with an Echelle spectrometer (with an effective spectral resolving power $\lambda/\Delta\lambda=4500$, certified by the producer of the instrument) equipped with a iCCD for time-resolved LIBS measurements. The measurements were performed both in single pulse, at 60 and 120 mJ laser energy, and in double-pulse regime (60+60 mJ with an interpulse delay of 2 μs). The laser beam(s) were focussed on the target surface by means of a 100 mm focal length lens; the lens to sample distance was set to 95 mm in order to improve the reproducibility of the breakdown. The LIBS signal was collected through an optical fibre (numerical aperture 0.22) set at 45° with respect to the laser beam axis, at about 10 mm from the laser spot. The LIBS measurements were performed as a function of the delay after the (second) laser pulse, to explore different plasma conditions (particle density, temperature and electron density). The LIBS spectra were acquired using a gate time of 500 ns, which provided a good signal to noise ratio, necessary for a precise measurement of the spectral line widths, at the same time guaranteeing that the plasma parameters (particle density, temperature and electron density) would remain quasi-stationary during the measurement time window.

The measurements of the line widths were performed through a Voigt fitting of the line profile; the Gaussian contribution due to the instrumental broadening was then deconvolved from the experimental FWHM in order to obtain the linewidth.

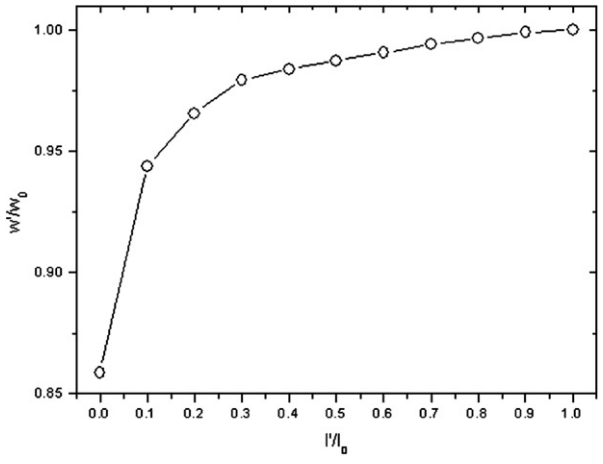

Fig. 2. Relative variation of the predicted linewidth of the Mn II line at 293.31 nm, as a function of the homogeneity parameter l'/l_0.

4.1. Characterization of the plasma

For all the samples considered, spectra were acquired in single and double pulse configuration and at different delay times after the (second) laser pulse. In particular, the delay range 1 to 3 μs was investigated: in fact, delays shorter than 1 μs caused the spectra to be dominated by continuum radiation, while at delays longer than 3 μs the ionic lines were too weak for our measurements. The spectra were analysed to derive the electron density and plasma temperature (in the assumption of LTE) corresponding to the experimental conditions here investigated.

The electron density of the laser-induced plasma was calculated by measuring the Stark broadening of the H_α line at 656.3 nm [12,13,27]. Hydrogen emission is always present in the LIBS spectra taken in ambient air, because of the water vapour due to the natural humidity of the air. The use of the H_α line for the measurement of the electron density has the definite advantage of providing a result which is not affected by self-absorption. Moreover, the linear Stark effect acting on the hydrogen atoms results in a large broadening of the lines which reduces the relative uncertainty of the measurement compared to the case of lines emitted by other elements [27].

The determination of the electron density was achieved using the tables compiled by Gigosos et al. [28]. The authors used computer simulations, including ion dynamics effects, obtaining a series of tables that provide the Stark FWHM of the Balmer-alpha, -beta and -gamma line profiles depending on the electron density, electron temperature and reduced mass of the emitter-ion system. As in case of Mn lines analysis, an homogenous plasma was assumed for the determination of the electron density.

In the Fig. 3, the measured values of the electron density are plotted as a function of the Mn concentration in the Fe–Mn alloys, for the three irradiation conditions used and acquisition delay of 1 μs after the (second) laser pulse. The error bars represent the uncertainty on the electron density determination due to the experimental errors in determining the H_α FWHM.

The electron density measurements do not show any particular trend with Mn percent concentration. The trend obtained for the spectra acquired at 2 and 3 μs delays (not shown here) is similar to the one in Fig. 3, with lower values of electron density. However, as reported in several papers by the authors [23,29,30], it is evident that the electron density in double pulse measurements is definitely lower than the one measured in single pulse LIBS at the same total energy (120 mJ), while it is comparable with the electron density measured in single pulse configuration and just 60 mJ of laser energy.

The plasma temperature was measured using the Saha–Boltzmann plot method. The Saha–Boltzmann plot is a generalization of the Boltzmann plot method, based on the assumption of ionization equilibrium according to the Saha equation, which includes lines coming from different ionization stages of the same element for the determination of plasma temperature, given the knowledge of the plasma electron density (see Ref. [31] for more details). In this approach, because of the larger maximum difference of the upper level energies of the transitions considered, a considerable reduction of the fitting error is obtained with respect to the usual Boltzmann plot method. A set of neutral and ionized, non resonant Fe lines was used for the measurements (see Table 1). To build the Saha–Boltzmann plot, the line integral intensities were used, obtained by best fitting of the lines with Voigt functions and corrected for the spectral efficiency of the detection apparatus.

Table 1
Spectral parameters of the lines used for plasma temperature determination

Wavelength (nm)	Species	A_{ki} (s^{-1})	g_i	g_k	E_i (cm^{-1})	E_k (cm^{-1})
259.84	Fe II	1.3×10^8	6	8	3.85×10^2	3.89×10^4
261.19	Fe II	1.1×10^8	8	8	3.85×10^2	3.87×10^4
261.38	Fe II	2.0×10^8	2	4	8.62×10^2	3.91×10^4
273.96	Fe II	1.9×10^8	8	8	7.96×10^3	4.44×10^4
381.58	Fe I	1.3×10^8	7	9	1.20×10^4	3.82×10^4
382.04	Fe I	6.7×10^7	9	11	6.93×10^3	3.31×10^4
407.17	Fe I	7.7×10^7	5	5	1.30×10^4	3.75×10^4
426.05	Fe I	3.2×10^7	11	11	1.94×10^4	4.28×10^4
432.58	Fe I	5.0×10^7	7	5	1.30×10^4	3.61×10^4
440.48	Fe I	2.75×10^7	9	7	1.26×10^4	3.53×10^4

Fig. 4 shows the values of plasma temperature obtained for the same conditions as in Fig. 3.

The experimental uncertainties on temperature calculation are of the order of 5%, coming mainly from the uncertainties of the electron density and the fitting of the line profiles. Although a careful choice of the Fe emission lines was performed, in order to reduce the effect of self-absorption on the same, the high concentration of iron in the samples (70–94%) could still produce self-absorption effects and, consequently, errors in the determination of the plasma temperature. In the actual experimental conditions of this paper, however, the application of the theoretical procedure described in Section 2.2 allows to determine that the effect of self-absorption is negligible for neutral lines and minimal for singly ionised Fe lines. This effect produces a slight systematic underestimation of the electron temperature (of the order of 3%) which is within the error determined by the uncertainty of the experimental data.

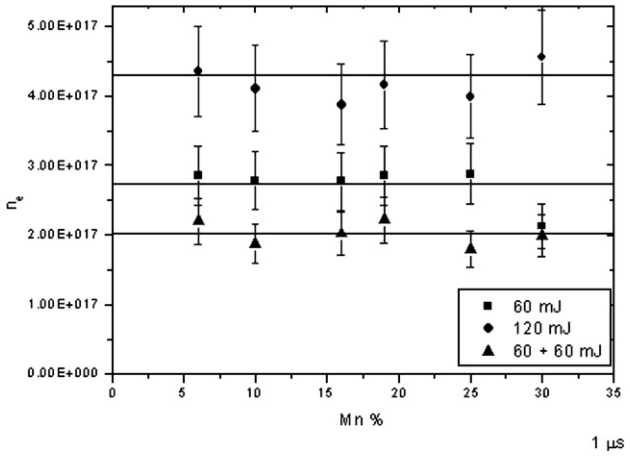

Fig. 3. Electron density as a function of the Mn concentration in the Fe–Mn alloy, measured in: single pulse configuration, laser energy 60 mJ (squares); single pulse configuration, laser energy 120 mJ (circles) and in double pulse configuration, laser energy 60 mJ per pulse, pulse separation 2 μs (triangles). The acquisition is started 1 μs after the (second) laser pulse.

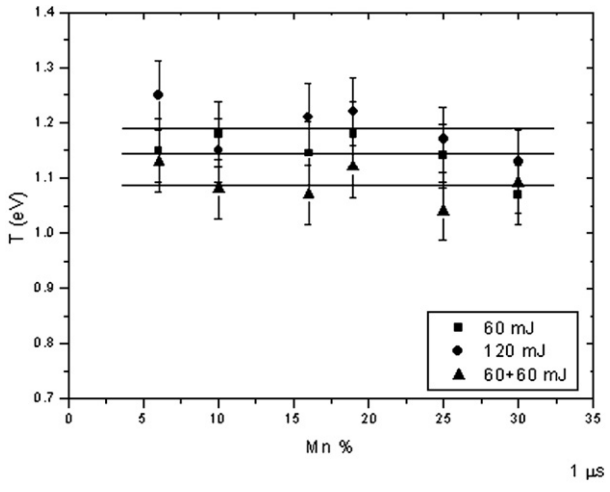

Fig. 4. Plasma temperature as a function of the Mn concentration in the Fe–Mn alloys, measured in: single pulse configuration, laser energy 60 mJ (squares); single pulse configuration, laser energy 120 mJ (circles) and in double pulse configuration, laser energy 60 mJ per pulse, pulse separation 2 μs (triangles). The acquisition is started 1 μs after the (second) laser pulse.

As in the case of electron density, no specific trend of the plasma temperature on Mn (and, consequently, on Fe) concentration in the alloy is recognizable. By comparing single and double pulse irradiation, it also turns out that the temperature is lower in single-pulse configuration. Similar results were obtained, for example, in Ref. [30]. This trend is confirmed by the analysis of the spectra acquired at delays of 2 and 3 μs (not shown here). As a result of the characterization described in the previous section, the plasma conditions corresponding to the shortest investigated delay (1 μs) were chosen for the measurement of the line broadening of both neutral and singly ionised Mn lines. In these experimental conditions the lines corresponding to both the ionisation stages of Mn show a substantial Stark broadening (it is advisable to process line profiles with as high FWHM as possible, in order to reduce the experimental uncertainty due to the fitting procedure) and the plasma temperature is relatively high. In fact, the higher the plasma temperatures, the smaller is the effect of self absorption (see discussion below).

4.2. Measurement of Stark coefficients of singly ionized Mn lines

As an example, the results of the measurement on the Mn II lines at 260.6 nm, 293.3 nm and 344.2 nm are reported in Fig. 5a–c as a function of the Mn weight percent concentration in the Fe–Mn alloy, for the different experimental conditions used (single pulse 60 mJ, single pulse 120 mJ, double pulse 60+60 mJ) and delay of 1 μs after the (second) laser pulse. The acquisition gate is 500 ns. To facilitate the comparison with the data already published [14,20], we reported the result of the measures as the HWHM (half width at half maximum) of the line in Å (after deconvolution of the Gaussian component introduced by the instrumental broadening) rescaled at the electron density of 10^{17} cm^{-3}.

According to Eq. (9), the measured width of the emission lines depends on the Self-Absorption coefficient; consequently, also the calculated 'apparent' Stark coefficients $\overline{w}_s$ shows the same dependence, i.e.

$$\overline{w}_s = w_s(\mathrm{SA})^{-0.54} \tag{10}$$

where w_s is the 'true' Stark coefficient (see Eqs. (1) and (2)) measured in conditions of low self-absorption. Using the expression of SA given in Eq. (7), we have

$$\overline{w}_s = w_s\left[\frac{\left(1-e^{-\kappa(\lambda_0)l}\right)}{\kappa(\lambda_0)l}\right]^{-0.54} \tag{11}$$

When the plasma opacity $\kappa(\lambda_0)l$ is low, the expression in Eq. (11) can be expanded in series

$$\overline{w}_s \approx w_s\left(1+\frac{0.54}{2}k(\lambda_0)l - O\left((k(\lambda_0)l)^2\right)\right) \tag{12}$$

The apparent Stark coefficient thus depends linearly, at least for low to moderate self-absorption, on the plasma opacity. The plasma opacity, in turns, depends linearly on the concentration

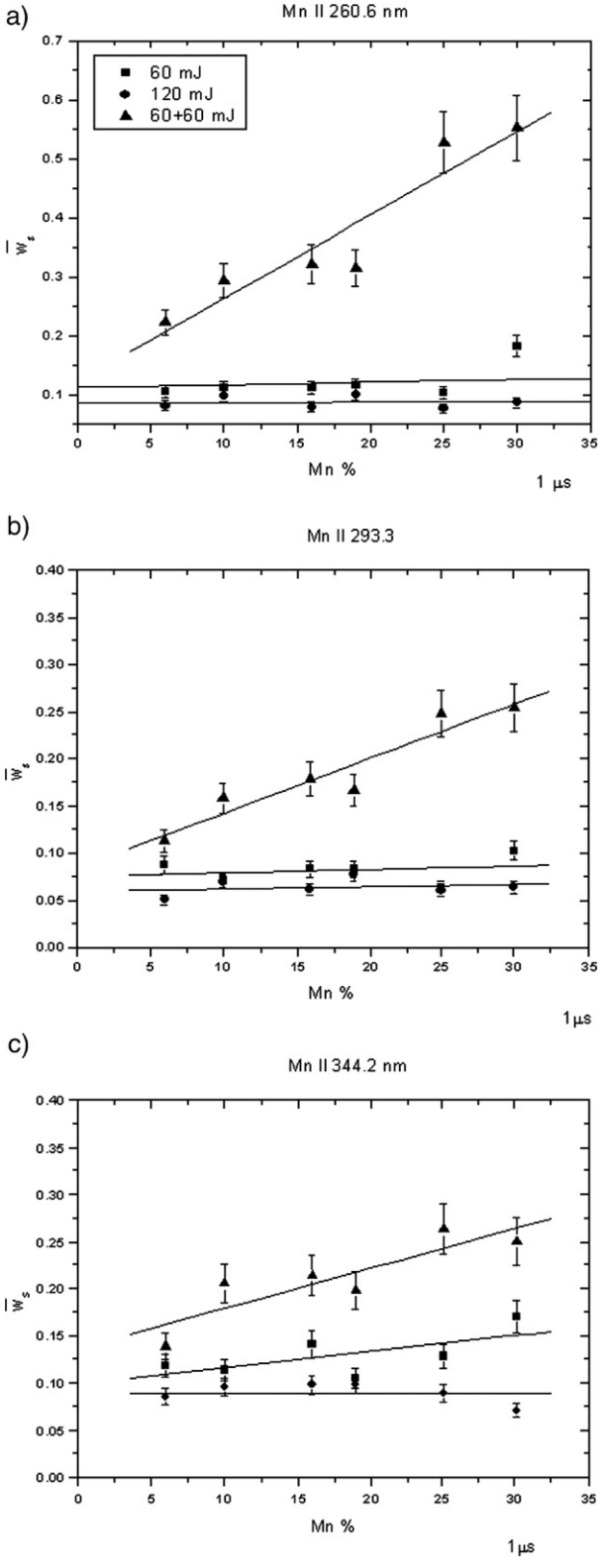

Fig. 5. Apparent Stark broadening parameter, as a function of the Mn weight percent in the alloy, in single pulse configuration, laser energy 60 mJ (squares), single pulse configuration, laser energy 120 mJ (circles) and in double pulse configuration, laser energy 60 mJ per pulse, pulse separation 2 μs (triangles). The acquisition is started 1 μs after the (second) laser pulse. a) MnII line at 260.6 nm; b) MnII line at 293.3 nm; c) MnII line at 344.2 nm.

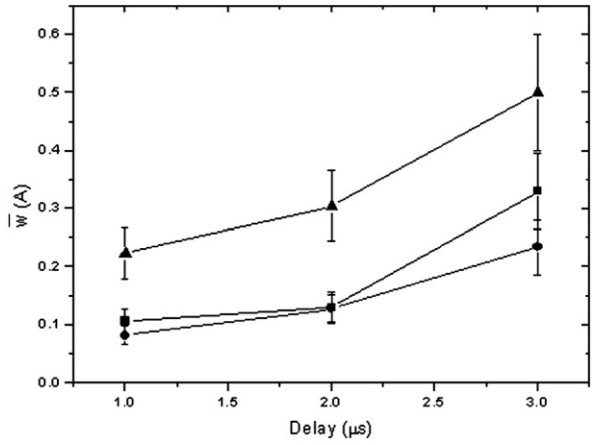

Fig. 6. Variation of the apparent Stark broadening parameter of the Mn II line at 260.6 nm, with the acquisition delay, for the sample with 6% concentration of Mn in the Fe–Mn alloy. Squares: single pulse configuration, laser energy 60 mJ; circles: single pulse configuration, laser energy 120 mJ; Triangles: double pulse configuration, laser energy 60 mJ per pulse, pulse separation 2 μs.

of the element of interest (see Eq. (5)). The extrapolation of the linear best-fit line to zero concentration (where self-absorption effects are negligible and SA = 1) would thus coincide with the w_s parameter defined in Eqs. (1) and (2).

It is clear from Fig. 5 that self-absorption effects make the apparent Stark coefficient of the emission lines larger than the 'true' one, according to the predictions of Eq. (12). This effect appears particularly important in double pulse LIBS measurements, as already reported by the authors in ref. [12,13]; in fact, the increase of ablated mass obtained in double pulse configuration also increases the optical opacity of the line. The self absorption effects increase with the increase of the Mn concentration in the Fe–Mn alloy. On the contrary, the line width seems to be relatively constant with the Mn concentration in the range considered for measurements performed in single pulse configuration. It also appears that the Mn lines obtained in single pulse LIBS configuration at 60 mJ energy are slightly wider than the ones obtained at 120 mJ. Although the separation between the two sets of data is close to the experimental error, this behaviour could be explained with the slightly lower plasma temperature obtained at lower laser energy (see Fig. 4). In fact, even small variation of the plasma excitation conditions are effective in increasing (lower temperatures) or decreasing (higher temperatures) the self-absorption effects. The temperature variation of the Stark broadening coefficient, on the contrary, is expected to produce a much lower effect and does not appear to justify the systematic difference between the two sets of data obtained at a laser energy of 60 and 120 mJ.

The self-absorption effects increase with increasing the acquisition delay, since the plasma expands and cools down. Fig. 6 shows the temporal behaviour of the apparent Stark coefficient of the Mn II line at 260.6 nm with the acquisition delay, in the different experimental configurations, at 6% concentrations of Mn in the Fe–Mn alloy.

Note that the apparent increase of the linewidth with the acquisition delay, especially in double pulse LIBS configuration, again is larger of what is expected considering the typical variation of the Stark coefficient with temperature [5–10]; therefore, the effect is dominated by the increase of self-absorption.

In principle, an evaluation of the Stark broadening of the Mn lines of interest could be obtained from Eq. (12), through a linear extrapolation of the dependence of the experimentally measured Stark broadening at zero Mn concentration. However, the error on linear fit in this procedure might be quite high. It is clear from the figures that the zero concentration extrapolation of the broadening obtained in strongly self-absorbed conditions (double pulse) does not always coincide with the same value obtained in low self-absorption conditions (single pulse). From the analysis of the experimental data, it thus seems that the best operating conditions for measuring the Mn lines linewidth correspond to single pulse at 120 mJ energy, with an acquisition delay of 1 μs. The Stark broadening coefficient of the Mn lines here considered were obtained using this experimental configuration. In these conditions, the HWHM of the Mn II 260.6 nm at 10^{17} e/cm^3 can be estimated as 0.09 ± 0.01 A. The estimated error comes mainly from the uncertainty in the experimental data which, according to the discussion of Section 3, is dominant on the effects of plasma inhomogeneity and non-stationariety.

By applying the same approach to other Mn II lines, we can obtain an experimental measurement of their Stark coefficients at element concentrations and plasma conditions which minimize the self-absorption effects. The corresponding results

Table 2
Comparison between theoretical and experimental Stark coefficients for the Mn II lines considered in this paper (the broadening measured in this paper were measured at an electron density $n_e = 4.3 \times 10^{17}$ cm^{-3} and then rescaled to $n_e = 10^{17}$ cm^{-3} according to Eq. (2))

Wavelength (nm)	Configuration (NIST, Ref. [24])	w_s exp. (Å) (this work)	w_s exp. (Å) (Djeniže et al. Ref. [14])	w_s Theor. (Å) (10,000 K, Ref. [20])	w_s Theor. (Å) (50,000 K, Ref. [20])
259.4	$3d^5(^6S)4s$–$3d^5(^6S)4p$	0.08 ± 0.01	0.07 ± 0.01	0.016	0.013
260.6	$3d^5(^6S)4s$–$3d^5(^6S)4p$	0.09 ± 0.01	0.075 ± 0.01	0.016	0.013
293.3	$3d^5(^6S)4s$–$3d^5(^6S)4p$	0.065 ± 0.01	0.08 ± 0.01	0.043	0.019
293.9	$3d^5(^6S)4s$–$3d^5(^6S)4p$	0.075 ± 0.01	0.06 ± 0.01	0.043	0.019
294.9	$3d^5(^6S)4s$–$3d^5(^6S)4p$	0.075 ± 0.01	0.08 ± 0.01	0.043	0.019
344.2	$3d^6$–$3d^5(^6S)4p$	0.090 ± 0.01	0.105 ± 0.01		
348.3	$3d^6$–$3d^5(^6S)4p$	0.065 ± 0.01	0.10 ± 0.01		
261.0	N.A.	0.065 ± 0.01	0.04 ± 0.01		
270.2	N.A.	0.045 ± 0.01	0.065 ± 0.01		

The electronic configuration are from NIST Atomic on-line database, Ref. [24] (N.A. = not available).

for the Stark coefficients are shown in Table 2 where a comparison with the data already available is immediate.

The Table shows that the our results, obtained from a LIBS plasma, are coherent with the experimental measurements made by Djeniže et al. [14]. The agreement seems satisfactory considering the different plasma temperatures in the two experiments (50,000 K in Djeniže et al., around 10,000 K in this work). As in the case of the Djeniže data, also the LIBS measurements leads to a discrepancy with the calculated theoretical values ranging from a factor of 1.5 to a factor of about 6.

4.3. Measurement of Stark coefficients of neutral Mn lines

At the best of our knowledge, no theoretical or experimental work on the emission lines broadening of neutral Mn is present in the literature. Using the same approach applied for Mn II, we were able to estimate, for the first time, the Stark broadening coefficients for several neutral Mn lines. The dependence of the apparent Stark coefficient with the Mn percent concentration is shown in Fig. 7 below, for single pulse (60 and 120 mJ) and double pulse (60+60 mJ) LIBS configurations for two lines. Note that in this case the experimental data are rescaled at the electron density $n_e = 10^{16}$ cm^{-3}, according to Eq. (1).

The corresponding extrapolated results are shown in Table 3.

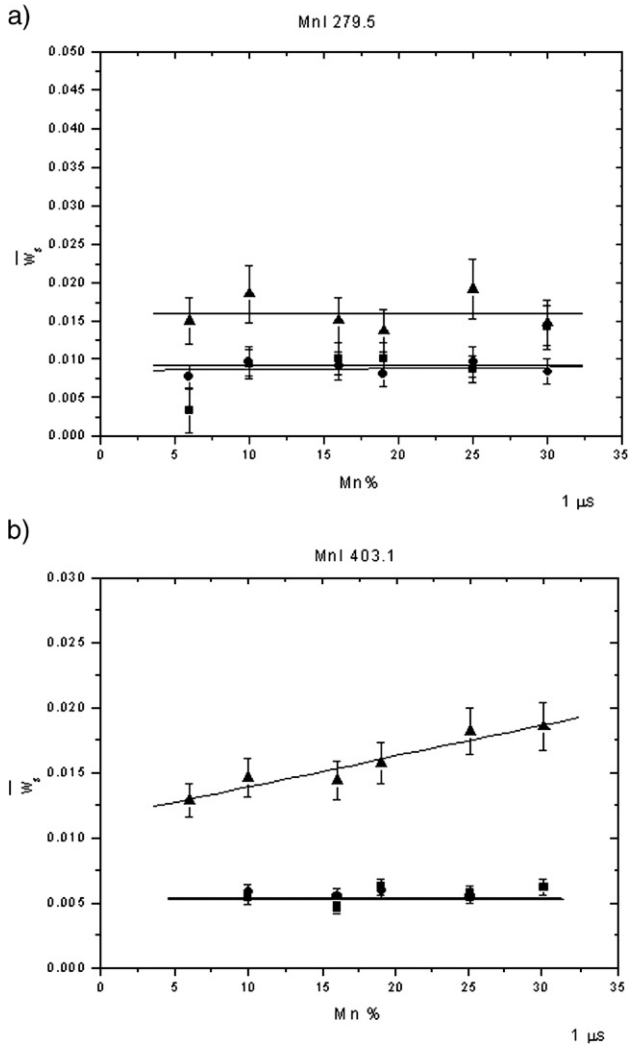

Fig. 7. Variation of the apparent Stark broadening parameter of the Mn I lines with the concentration of Mn in the Fe–Mn alloy. Squares: single pulse configuration, laser energy 60 mJ; circles: single pulse configuration, laser energy 120 mJ; Triangles: double pulse configuration, laser energy 60 mJ per pulse, pulse separation 2 µs. a) Mn I line at 279.5 nm; b) Mn I line at 403.1.

Table 3
Measured Stark coefficients for the Mn I lines considered (the broadening was measured at an electron density $n_e = 4.3 \times 10^{17}$ cm^{-3} and then rescaled to $n_e = 10^{16}$ cm^{-3} according to Eq. (1))

Wavelength (nm)	Configuration	w_s (Å) (this work)
279.5	$3d^5 4s^2$–$3d^5(^6S)4s4p(^1P°)$	0.008±0.001
403.1	$3d^5 4s^2$– $3d^5(^6S)4s4p(^3P°)$	0.005±0.001
403.3	$3d^5 4s^2$– $3d^5(^6S)4s4p(^3P°)$	0.006±0.001
404.1	$3d^6(^5D)4s$– $3d^6(^5D)4p$	0.006±0.001
476.2	$3d^6(^5D)4s$– $3d^6(^5D)4p$	0.018±0.001

The electronic configuration are from NIST Atomic on-line database, Ref. [24].

5. Conclusion

In this paper we have presented the experimental measurement of the Stark coefficients of 9 Mn II lines and – for the first time – 5 Mn I lines. The results presented were obtained from a laser-induced plasma as the emitting source. Time-resolved spectra were acquired via the LIBS technique on Fe–Mn samples with Mn concentration ranging from 30 to 6%. The measured coefficients of MnII lines are coherent with previous measurements performed by Djeniže et al. [14]. The measured Stark coefficients are a resource for a number of LIBS applications, for example the quick estimate of the degree of self-absorption of these lines, as proposed by the authors in recent papers [12,32].

Acknowledgements

This research is part of the activities of the SAILORMAN (Southern American–Italian LIBS-Oriented Research for Material Analysis Network), a cooperative research network connecting LIBS laboratories in Argentina (CIOP, La Plata and Universidad Nacional del Centro in Tandil), Mexico (Universidad Nacional Autónoma de México), Brazil (Universidade Federal Fluminense) and Italy (ALS Lab.-CNR in Pisa).

References

[1] J.T. Davies, J.M. Vaughan, A new tabulation of the Voigt profile, Astrophys. J. 137 (1963) 1302–1317.
[2] H.O. Di Rocco, Systematic trends and relevant atomic parameters for Stark line shifts and widths, Spectrosc. Lett. 23 (1990) 283–292.
[3] C. Colon, G. Hatem, E. Verdugo, P. Ruiz, J. Campos, Measurement of the Stark broadening and shift parameters for several ultraviolet lines of singly ionized aluminum, J. Appl. Phys. 73 (1993) 4752–4758.
[4] A.N. Mostovych, L.Y. Chan, K.J. Kearney, D. Garren, C.A. Iglesias, M. Klapisch, F.J. Rogers, Opacity of dense, cold, and strongly coupled plasma, Phys. Rev. Lett. 75 (1995) 1530–1533.
[5] N. Konjevic, J.R. Roberts, A critical review of the Stark widths and shifts of spectral lines from non-hydrogenic atoms, J. Phys. Chem. Ref. Data 5 (1976) 209–257.

[6] N. Konjevic, W.L. Wiese, Experimental Stark widths and shifts for non-hydrogenic spectral lines of ionized atoms (a critical review and tabulation of selected data), J. Phys. Chem. Ref. Data 5 (1976) 259–308.
[7] N. Konjevic, M.S. Dimitrijevic, W.L. Wiese, Experimental Stark widths for spectral lines of neutral atoms (a critical review of selected data for the period 1976 to 1982), J. Phys. Chem. Ref. Data 13 (1984) 619–647.
[8] N. Konjevic, M.S. Dimitrijevic, W.L. Wiese, Experimental Stark widths for spectral lines of positive ions (a critical review and tabulation of selected data for the period 1976 to 1982), J. Phys. Chem. Ref. Data 13 (1984) 649–686.
[9] N. Konjevic, M.S. Dimitrijevic, W.L. Wiese, Experimental Stark widths for spectral lines of neutral and ionized atoms (a critical review of selected data for the period 1983 through 1988), J. Phys. Chem. Ref. Data 19 (1990) 1307–1385.
[10] N. Konjevic, A. Lesage, J.R. Fuhr, W.L. Wiese, Experimental Stark widths for spectral lines of neutral and ionized atoms (a critical review of selected data for the period 1989 through 2000), J. Phys. Chem. Ref. Data 31 (2002) 819–927.
[11] J. Bengoechea, J.A. Aguilera, C. Aragón, Application of laser-induced plasma spectroscopy to the measurements of Stark broadening parameters, Spectrochim. Acta Part B 61 (2006) 69–80.
[12] A.M. El Sherbini, Th.M. El Sherbini, H. Hegazy, G. Cristoforetti, S. Legnaioli, V. Palleschi, L. Pardini, A. Salvetti, E. Tognoni, Evaluation of self-absorption coefficients of aluminum emission lines in laser-induced breakdown spectroscopy measurements, Spectrochim. Acta Part B 60 (2005) 1573–1579.
[13] A.M. El Sherbini, Th. El Sherbini, H. Hegazy, G. Cristoforetti, S. Legnaioli, L. Pardini, V. Palleschi, A. Salvetti, E. Tognoni, Measurement of the Stark broadening of atomic emission lines in non-optically thin plasmas by laser-induced breakdown spectroscopy, Spectrosc. Lett. 40 (2007) 643–658.
[14] S. Djeniže, S. Bukvić, A. Srećković, D. Nikolić, The first measured Mn II and Mn III Stark broadening parameters, New Astron. 11 (2006) 256–261.
[15] G.P. Kopitsa, V.V. Runov, S.V. Grigoriev, V.V. Bliznuk, V.G. Gavriljuk, N.I. Glavatska, The investigation of Fe–Mn-based alloys with shape memory effect by small-angle scattering of polarized neutrons, Physica B 335 (2003) 134–139.
[16] T. Schneider, M. Acet, B. Rellinghaus, E. Wassermann, W. Pepperhoff, Antiferromagnetic Invar and anti-Invar in Fe–Mn alloys, Phys. Rev. B 51 (1995) 8917–8921.
[17] A. Borgenstam, M. Hillert, The driving force for Lath and Plate martensite and the activation energy for isothermal martensite in ferrous alloys, J. Phys. IV 7 (1997) C5:23–C5:28.
[18] S.M. Cotes, A. Fernández Guillermet, M. Sade, Gibbs energy modelling of the driving forces and calculation of the fcc/hcp martensitic transformation temperatures in Fe–Mn and Fe–Mn–Si alloys, Mater. Sci. Eng. A 273–275 (1999) 503–506.
[19] A. Baruj, A. Fernández Guillermet, M. Sade, Effects of thermal cycling and plastic deformation upon the Gibbs energy barriers to martensitic transformation in Fe–Mn and Fe–Mn–Co alloys, Mater. Sci. Eng. A 273–275 (1999) 507–511.
[20] L.C. Popović, M.S. Dimitrijević, The electron impact broadening parameters in hot star atmospheres: Mn II, Mn III, Ga III, Ge III and Ge IV lines, Astron. Astrophys., Suppl. Ser. 128 (1998) 203–205.
[21] N. Konjevic, Plasma broadening and shifting of non-hydrogenic spectral lines: present status and applications, Phys. Rep. 316 (1999) 339–401.
[22] J. Bengoechea, C. Aragón, J.A. Aguilera, Asymmetric Stark broadening of the Fe I 538.34 nm emission line in a laser-induced plasma, Spectrochim. Acta Part B 60 (2005) 897–904.
[23] M. Corsi, G. Cristoforetti, M. Giuffrida, M. Hidalgo, S. Legnaioli, V. Palleschi, A. Salvetti, E. Tognoni, C. Vallebona, Three-dimensional analysis of laser induced plasmas in single and double pulse configuration, Spectrochim. Acta Part B 59 (2004) 723–735.
[24] Yu. Ralchenko, F.-C. Jou, D.E. Kelleher, A.E. Kramida, A. Musgrove, J. Reader, W.L. Wiese, K. Olsen, NIST Atomic Spectra Database (version 3.1.3), National Institute of Standards and Technology, Gaithersburg, MD, 2007, [Online]. Available: http://physics.nist.gov/asd3 [2007, October 2].
[25] Kurucz database. [Online]. Available: http://cfa-www.harvard.edu/amp/ampdata/kurucz23/sekur.html [2007, October 2].
[26] A. Bertolini, G. Carelli, F. Francesconi, M. Francesconi, L. Marchesini, P. Marsili, F. Sorrentino, G. Cristoforetti, S. Legnaioli, V. Palleschi, L. Pardini, A. Salvetti, Modì: a new mobile instrument for in situ double-pulse LIBS analysis, Anal. Bioanal. Chem. 385 (2006) 240–247.
[27] A.M. El Sherbini, H. Hegazy, Th.M. El Sherbini, Measurement of electron density utilizing the Hα-line from laser produced plasma in air, Spectrochim. Acta Part B 61 (2006) 532–539.
[28] M.A. Gigosos, V. Cardeñoso, New plasma diagnosis tables of hydrogen Stark broadening including ion dinamics, J. Phys. B: At. Mol. Opt. Phys. 29 (1996) 4795–4838.
[29] G. Cristoforetti, S. Legnaioli, V. Palleschi, A. Salvetti, E. Tognoni, Influence of ambient gas pressure on laser-induced breakdown spectroscopy technique in the parallel double-pulse configuration, Spectrochim. Acta Part B 59 (2004) 1907–1917.
[30] G. Cristoforetti, S. Legnaioli, V. Palleschi, A. Salvetti, E. Tognoni, Characterization of a collinear double pulse Laser-Induced Plasma at several ambient gas pressures by spectrally-and time-resolved imaging, Appl. Phys. B 80 (2005) 559–568.
[31] S. Yalcin, D.R. Crosley, G.P. Smith, G.W. Faris, Influence of ambient conditions on the laser air spark, Appl. Phys. B 68 (1999) 121–130.
[32] F. Bredice, F.O. Borges, H. Sobral, M. Villagran-Muniz, H.O. Di Rocco, G. Cristoforetti, S. Legnaioli, V. Palleschi, L. Pardini, A. Salvetti, E. Tognoni, Evaluation of self-absorption of manganese emission lines in Laser Induced Breakdown Spectroscopy measurements, Spectrochim. Acta Part B 61 (2006) 1294–1303.